Ductility and energy dissipation of perforated steel plate shear walls

R Abd Samat, D Tahir, A B Fadzil and S Abu Bakar

School of Civil Engineering, Faculty of Engineering, Universiti Teknologi Malaysia, 81310 UTM Skudai, Johor, Malaysia.

Email: roslida@utm.my

Abstract. Steel plate shear wall (SPSW) that consists of boundary elements and steel plate, has been used as a structural system to resist lateral loads such as strong wind and earthquake. The capability of SPSW to resist a relatively strong earthquake has been tested in an actual earthquake when a 35-story high rise building that employed SPSW stood still during 1995 Kobe earthquake while a nearby building collapsed during the catastrophe. The need for serviceability such as piping, duct for air conditioning, heating and ventilation as well as passageway requires SPSW to be perforated. Despite the expanding research on SPSW, there is a scarcity in the research on the effect of perforations on the performance of the SPSW. The objective of this research is to determine how openings of different sizes and orientations influence energy dissipation, shear load capacity, and ductility ratio of SPSW. Earthquake resistant building must have adequate energy dissipation capacity and ductility. Analysis was carried out on six SPSW models where three of them were denoted as Model A series. These models differ in the area of the openings. The rest of the models were denoted as Model B series which have the exact area of perforation, but different orientation. In both series, ASTM A36 steel was used for the plate and ASTM A992 steel was used for the boundary elements. The results were obtained with the aid of ABAQUS software application. Lateral loads were allowed in a cyclic orientation applied to a single side of the structure following the protocols of ATC 24. It is concluded that certain sizes of openings enhance the energy dissipation and ductility ratio. Model B3 which has the smallest dimension of the opening perpendicular to the load has the largest energy dissipation and shear load capacity but, has the smallest ductility.

1. Introduction

In the design of high-rise buildings, lateral loads form an important and inseparable part of the design consideration. Steel plate shear walls (SPSWs) are structural element that has been, and still being utilized as tall building systems that resist lateral load. SPSWs are meant to carry only lateral loads in a structure, whereas all gravity loads are transferred to other structural elements, such as beams, columns and load bearing walls. The development of tension areas in unstiffened SPSWs enables SPSWs to have good ductility and high dissipation of energy during the exertion of cyclic loading [1-3]. Common types of lateral loads are wind loads and seismic loads which are cyclic loads. In the recent decades, steel plate shear walls (SPSWs) are known to be very effective in resisting the lateral load which includes wind and seismic load.

A typical SPSW system is composed of vertical steel plates surrounded by vertical and horizontal boundary elements (beams and columns) [4]. The advantages of SPSWs over other tall building

systems are lower foundation cost due to the light weight of the SPSWs, less steel consumption, better performance, easy to design, fast to construct and more usable area in buildings [5]. SPSW has lighter weight in comparison with concrete's weight. The strength and ductility of steel plate shear walls make them quite suitable in buildings located in seismic high-risk regions. In general, SPSWs are effective and economical systems to resist lateral loads acted to buildings with 15 – 40 stories [6]. SPSWs can be used not only for the design of new buildings but also, to retrofit existing buildings [7,8].

The lateral stiffness of SPSW system must be computed accurately as the lateral deflection of the system must comply the drift limits specified in the design code. Both the initial elastic stiffness and the post-buckling stiffness of the SPSW system must be considered in the calculation of the lateral stiffness of a SPSW system [3]. Either approximate hand method which applies the deep beam theory or computer method which applies the truss analogy can be used to calculate the lateral stiffness of SPSW as both methods have acceptable accuracy compared to finite element and strip methods [3]. The strip method uses a series of inclined tensile strips to represent tension field that forms in buckled unstiffened SPSW [9]. The hysteretic behaviour and the shear capacity of the SPSW can be predicted by employing Plate and Frame Interaction (PFI) method where the effect of plastic yielding of the infill steel plate and the surrounding frame as well as the shear buckling of the infill steel plate were incorporated [10]. The structural responses of the SPSW such as yield strength, yield displacement, ultimate strength, initial stiffness and secondary stiffness, of the SPSW is mostly influenced by the infill plate thickness followed by the beam size [11].

Openings or perforations in SPSWs in buildings are often needed due to architectural reasons as well as for man access requirements [5, 6]. Regardless of the known fact that opening reduced the stiffness and strength in panels, it is essential to determine the degradation which relates to the size and location of the opening. [12]. The shear capacity of the SPSWs with centrally placed circular openings can be computed by using a linear reduction empirical factor ($1-D/d$) to the strength and stiffness of similar unperforated panel, where D is the opening diameter and d is the panel height [13].

The reduced strength and stiffness of perforated SPSW limit the deformation demand induced to frame member by thick infill steel plate [1], which allows the usage of thicker infill steel plate during the unavailability of thin steel plate in the market [14]. Interestingly, the existence of vertical slots in the web of horizontal boundary element increased the ductility of conventional SPSW [15]. Further, large opening of the SPSW can be provided by the use of coupled steel plate shear wall. The adoption of very large concrete-filled steel tubes (CFT's) as edge column of the coupled steel plate shear wall allow the edge column to remain elastic while the seismic components (infill steel plate, interior vertical boundary elements and horizontal beams) are yielding and dissipating energy and thus, is effective to resist seismic [16].

Despite the numerous research on unstiffened conventional SPSWs, limited research had been performed on SPSWs with various kinds of openings [6]. Large rectangular openings in SPSWs are often required for passageway, window and entrances to stairs and lifts. With the existence of large rectangular openings in SPSW, several characteristics of SPSW such as stiffness, buckling, and deformation vary. The hysteretic behaviour of the SPSW allows energy dissipation of the input energy imposed to a building due to the lateral loads. Therefore, it is crucial for the designer to know the parameters of the perforations which will maximize the energy dissipation of the SPSW. The objective of this study is to obtain the hysteresis curves of SPSWs of the same dimensions but with different opening dimensions and opening orientations which allows the determination of the change of its energy dissipation, ductility ratio and shear load capacity. This study is essential to provide guidance to architects and structural engineers to help them designing an optimum SPSWs which can effectively carry lateral loads on a structure with minimum cost. An analysis of steel plate shear walls with rectangular openings using the software ABAQUS is performed in this research.

2. Methodology

Analysis was performed on six steel plate shear wall (SPSW) models that were 4 m high and 4 m wide. The SPSWs were composed of steel plate with 5mm thickness and W360 mm x 33 kg/m wide flange I-beam as boundary elements. The steel plate and the boundary elements were made from A36 steel and A992 steel, respectively. The six models were divided into two groups: group A and B as shown in Figure 1. Group A's models consist of centralized perforations of an increasing size. Model A1 has the smallest size of opening, followed by model A2 and model A3 with the largest opening size. Group B's models however have a similar area of opening but with a different orientation. B1 has a perfect square shape perforation, whereas the perforations in B2 and B3 are rectangular in shape, vertical in B1 and horizontal orientation in the case of B2. Table 1 tabulates the dimensions of the perforation in both group A and B models.

The lateral cyclic load was applied at the top of the models and was in accordance with the protocols of ATC 24 (Guidelines for Cyclic Seismic Testing of Components of Steel Structures). The concept was to allow movement or deformation of the SPSW system in the lateral direction with the amplitude given by the ATC 24 as shown in Figure 2. The load is automatically generated by the software application which is Abaqus. The amplitude rises and falls ranging between positive and negative deformations values and it returns to zero after every step. This requires load to be imposed to the element throughout the loading steps. When the steps are completed, the program generates the cyclic loading required for each cycle. The data are then transferred to Excel sheet to facilitate the graphical presentation.

Table 1. Dimensions the perforation of all models.

Models		Height (m)	Width (m)	Area (m^2)
A	1	0.50	0.50	0.25
	2	0.75	0.75	0.56
	3	1.00	1.00	1.00
B	1	0.87	0.87	0.75
	2	1.50	0.50	0.75
	3	0.50	1.50	0.75

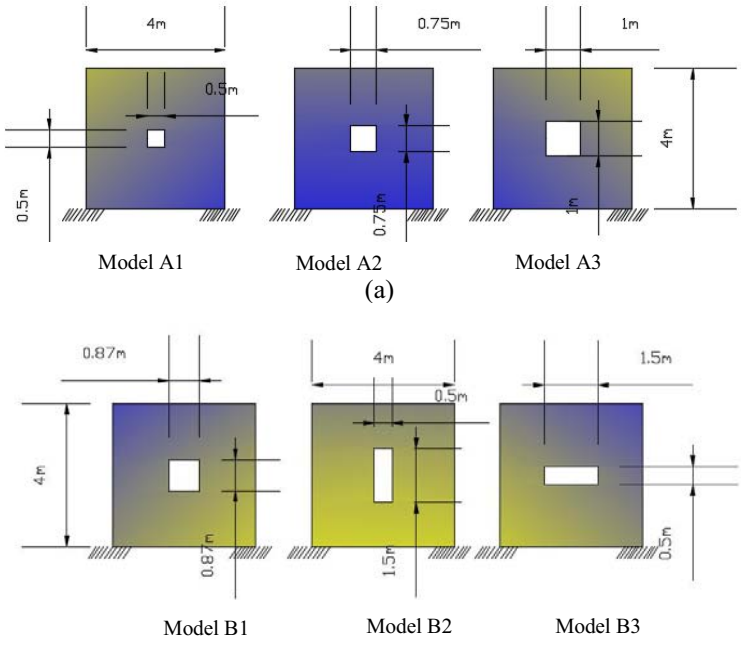

Figure 1. Dimension of models in (a) Group A and (b) Group B.

Hysteresis graphs were plotted based on the lateral displacements and the corresponded values of the lateral loads applied. Energy dissipation of each model was obtained by calculating the area of all loops in the hysteresis graph by using Excel spread sheet template. Ductility ratios was calculated by dividing the maximum displacement though out the cyclic load application period by the displacement at yield for each model. The results which are energy dissipation, shear load capacity and ductility of all models were compared to determine the behaviour of the parameters of interest when the size of the perforation was increased and when the orientation the perforation was changed.

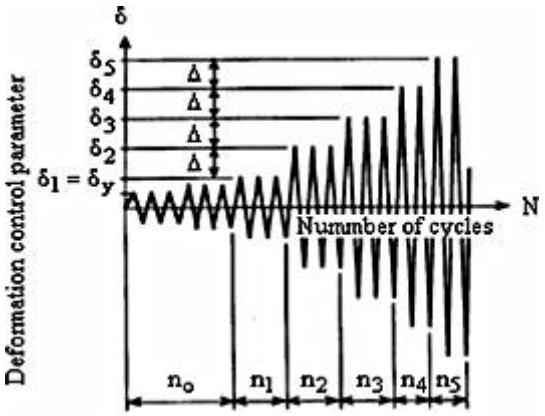

Figure 2. Deformation history for multiple step test as according to ATC24.

3. Results and discussion

Hysteretic curves of all models were compared to understand the behaviour of the models with variation of the perforations. Deformation and shear load capacity affect the values of energy dissipation and ductility ratio of these models.

3.1. Hysteresis behaviour

Hysteresis behavior of models A1, A2, and A3 are shown in Figures 3(a), 3(b) and 3(c) respectively. This set of models were analysed to determine the effect and the changes in the hysteretic behaviour when the area of the perforation is increased from 0.5m x 0.5m for A1 to 0.75m x 0.75m for A2, and 1.0 m x 1.0 m for model A3. Overall, the sequence or the paths of the hysteretic graphs are symmetrical except for model A2 which behaves in an unexpected unsymmetrical manner. A closer look of how model A2 deformed as in Figure 4(b) shows that out of plane buckling had occurred in model A2 when cyclic load was applied. The deformation or the displacement in the aforementioned is the highest in group A models despite the size of its perforation is not the largest among group A models. Model A3 which has the largest perforation had smaller value of displacement compared to model A2 as shown in Table 2. The smallest planar area of model A3 due to the large size of perforation had caused the molecules of A3 model to dislocate as in strain hardening condition, and thus model A3 became stiffer and had less displacement and did not buckle.

The hysteretic graphs of all models in group B are symmetrical and none of them experience out of plane buckling as shown in Figure 5(a), 5(b) and 5(c). The displacements of all models in group B were almost the same, but were larger than the control model (Table 2). In general, the existence of the opening allows larger displacement compared to the control model.

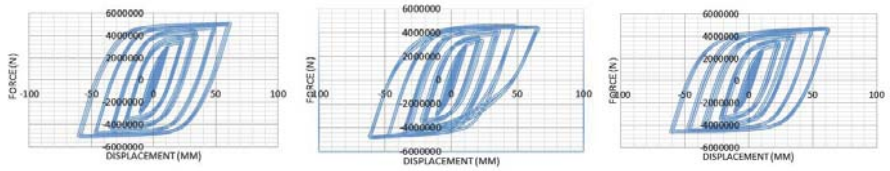

(a) (b) (c)

Figure 3. Hysteretic curve of (a) model A1, (b) model A2, (c) model A3.

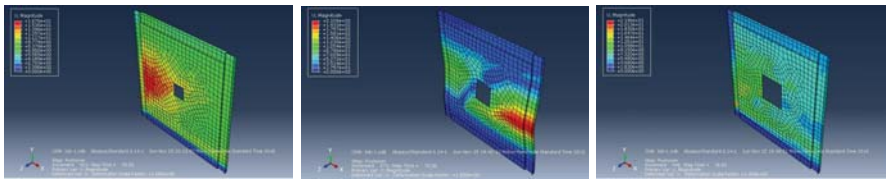

(a) (b) (c)

Figure 4. Deformed shape of model (a) A1 (b) A2 (c) A3.

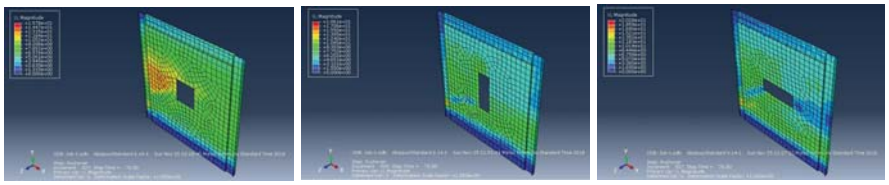

(a) (b) (c)

Figure 5. Deformed shape of model (a) B1 (b) B2 (c) B3.

Table 2. Maximum displacement of all models.

Group		A			B		Control
Model	A1	A2	A3	B1	B2	B3	
Displacement (mm)	61.60	65.40	61.34	62.59	61.72	62.00	58.17

3.2. Shear load capacity

The shear load capacity is opposite proportional with the size of opening as the results suggest for models in group A. The smaller the size of the opening is, the larger shear load it can endure (Figure 6(a)). Thus, Model A3 with the largest perforation has the smallest shear load capacity. But in the case of the models in group B, the result shows an interesting relationship where the shear load capacity maximizes with the smallest dimension of the perforation to which the load is perpendicular. Model B2 which had the largest dimension of the perforation to which the load is perpendicular had the least shear load capacity, while model B1 with square opening had similar results as model B3 (Figure 6(b)).

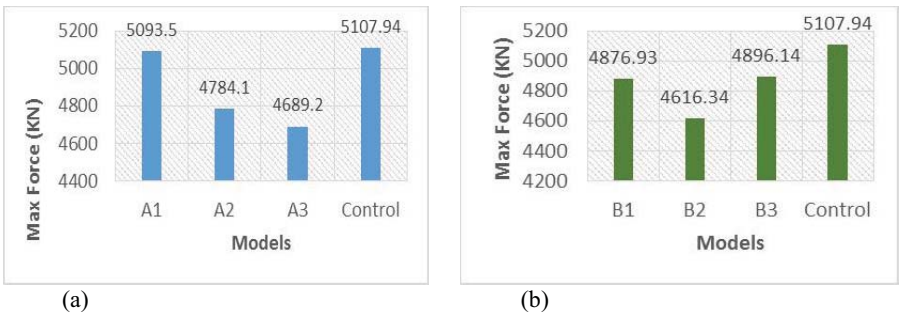

(a) (b)

Figure 6. Shear load capacities of (a) set A, (b) set B models.

3.3. Energy dissipation

In group A models, the cumulative energy dissipation exerts unexpected results where the model with no perforations provides less energy dissipation values than the A1 and A3 models which encapsulate a perforation of 0.5 m x 0.5 m and 1 m x 1 m opening size, respectively. Model A1 which has the smallest opening has the largest cumulative energy dissipation among all models while model A2 which experienced out of plane buckling had least energy dissipation capacity that is lower than the control model (Figure 7(a)).

Energy dissipation of models that had constant opening area but with alternating orientations and shapes of opening however show a consistent pattern (Figure 7(b)). SPSW gives more reliable energy dissipation results when the dimension of the opening perpendicular to the cyclic load is kept minimal. Model B3 which has a 0.5 m dimension of opening perpendicular to the load direction has the highest energy dissipation in contrast to the model with the longest dimension in the same position (B2) that provides the least energy dissipation capacity. Model B1 which is in between the aforementioned models in terms of the dimension comes in the middle roughly on the energy dissipation graph. Thus, when the perforation had smaller dimension that is perpendicular to the load direction, the SPSW will dissipate higher energy dissipation and vice versa when perforation had larger dimension that is perpendicular to the load. All models in set B had larger energy dissipation compared to control model.

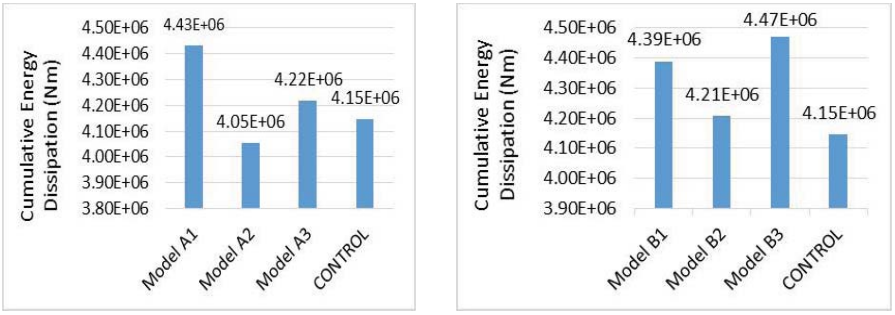

(a) (b)

Figure 7. Cumulative energy dissipation of (a) set A, (b) set B models.

3.4. Ductility

Ductility ratio is the ratio of the maximum displacement to that of the same structure at yield point. The ductility ratios in the models of this study are summarized in Table 3 and plotted in Figure 10. When the opening is the largest as in model A3, strain hardening had occurred and caused the model to become stiffer, and thus reduced the ductility ratio as shown in Figure 8(a). In the case of models in group B, the ductility is at its highest values when the shape of the opening is square, and it drops to the lowest value when the smaller dimension perpendicular to the load was adopted.

Table 3. Ductility ratio of all models.

Models		Maximum displacement (mm)	Displacement at yield (mm)	Ductility ratio
A	1	61.60	14.79	4.16
	2	65.40	15.70	4.17
	3	61.34	16.84	3.86
B	1	62.54	13.64	4.59
	2	61.72	14.73	4.19
	3	60.00	16.99	3.65
Control		58.17	14.07	4.14

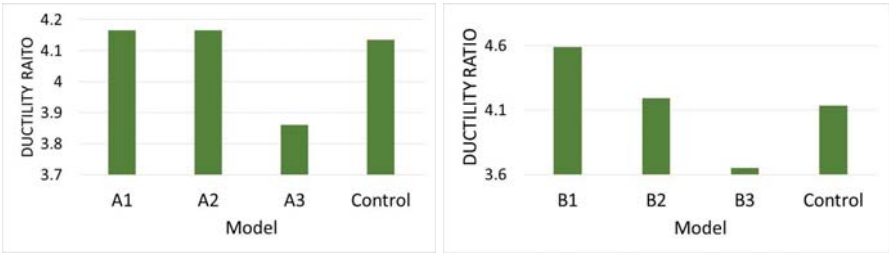

(a) (b)

Figure 8. Ductility ratios of models in (a) Group A, (b) Group B.

4. Conclusion

To conclude, the shear load capacity is inversely proportion with the size of the perforation. Model A1 which had the smallest perforation reduced the shear load capacity by only 0.3 percent. In terms of the orientation, square and horizontal perforation caused less than 5 percent of the reduction of the shear load capacity compared to the control model. Vertical perforation caused the shear load capacity to drop by about 10 percent.

Energy dissipation is increased by the existence of perforation except for model A2 which experienced out of plane buckling. Model A1 which has the smallest opening has the largest cumulative energy dissipation among group A models where energy dissipation was increased by 6.75 percent. Square and horizontal perforation increased energy dissipation by 6 percent and 8 percent, respectively, while the vertical perforation increased energy dissipation only by 1.4 percent.

Ductility ratio was unchanged in group A models compared to control model, except model A3, where ductility ratio was reduced by 6.8 percent as it became stiffer due to strain hardening. B3 models which had horizontal perforation had the largest reduction of ductility compared with the control model, which is by 11.8 percent.

Acknowledgement

The study was funded by the Ministry of Education Malaysia and Research Management Centre, Universiti Teknologi Malaysia under Fundamental Research Grant Scheme (FRGS) No. R.J130000.7851.5F052.

References

[1] Chan R, Albermani F and Kitipornchai S 2011 *Procedia Eng* **14** 675-679
[2] Astaneh-Asl A 2000 *Proceedings, U.S.-Japan Partnership for Advanced Steel Structures*
[3] Topkaya C and Atasoy M 2009 *Thin Wall Struct* **47** 827-835
[4] Barkhordari M A, Asghar Hosseinzade S A and Seddighi M 2014 *Asian J. Civ Eng* **15** 741-759
[5] Hosseinzadeh S A A and Tehranizadeh M 2012 *J Constr Steel* **77** 180–192
[6] Sabouri-Ghomi S and Mamazizi S 2015 *Thin Wall Struct* **86** 56–66
[7] Berman J W and Bruneau M 2003 *Technical Report No. MCEER-03-0001*
[8] Driver R G Kulak G L Kennedy D J L and Elwi A E 1998 *J Struct Eng* **124**
[9] Trompoch E W and Kulak G L 1987 *Cyclic and Static Behaviour of Thin Panel Steel Plate Shear Wall*
[10] Roberts T M and Ghomi S S 1991 *Thin Wall Struct* **12** 145-162
[11] Alhamaydeh M and Sagher A 2017 *7th International Conference on Modeling, Simulation, and Applied Optimization*
[12] Sabouri-Ghomi S, Ahouri E, Sajadi R, Alavi M, Roufegarinejad A, Bradford M A 2012 *J Constr Steel Res* **79** 91–100
[13] Roberts T M and Sabouri-Ghomi S 1992 *Thin Wall Struct* **14** 139-151
[14] Vian D and Bruneau M 2006 *4th International Conference on Earthquake Engineering*
[15] Asl M H and Safarkhani M 2017 *Thin Wall Struct* **116** 169-179
[16] Zhao Q and Astaneh-asl A 2004 *13th World Conference on Earthquake Engineering*